
Learning Decision Trees with Gradient Descent

Sascha Marton
Institute for Enterprise Systems
University of Mannheim
sascha.marton@uni-mannheim.de

Stefan Lüdtkke
ScaDS.AI
University of Leipzig
stefan.luedtke@uni-leipzig.de

Christian Bartelt
Institute for Enterprise Systems
University of Mannheim
christian.bartelt@uni-mannheim.de

Heiner Stuckenschmidt
Data and Web Science Group
University of Mannheim
heiner.stuckenschmidt@uni-mannheim.de

Abstract

Decision Trees (DTs) are commonly used for many machine learning tasks due to their high degree of interpretability. However, learning a DT from data is a difficult optimization problem, as it is non-convex and non-differentiable. Therefore, common approaches learn DTs using a greedy growth algorithm that minimizes the impurity locally at each internal node. Unfortunately, this greedy procedure can lead to suboptimal trees. In this paper, we present a novel approach for learning hard, axis-aligned DTs with gradient descent. The proposed method uses backpropagation with a straight-through operator on a dense DT representation to jointly optimize all tree parameters. Our approach outperforms existing methods on binary classification benchmarks and achieves competitive results for multi-class tasks.

1 Introduction

Decision trees (DTs) are one of the most popular machine learning models and are still frequently used today. In particular, with the growing interest in explainable artificial intelligence (XAI), DTs have regained popularity due to their interpretability. However, learning a DT is a difficult optimization problem, since it is non-convex and non-differentiable. Finding an optimal DT for a specific task is an NP-complete problem [19]. Therefore, the common approach to construct a DT based on data is a greedy procedure that minimizes the impurity at each internal node [8]. The algorithms that are still used today, such as CART [8] and C4.5 [34], were developed in the 1980s and have remained largely unchanged since then. Unfortunately, a greedy algorithm only yields to locally optimal solutions and therefore can lead to suboptimal trees, as we illustrate in the following:

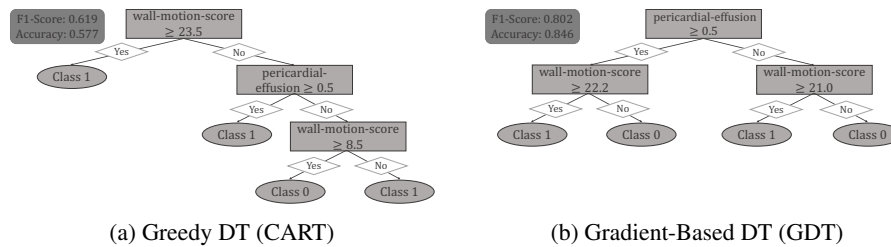


Figure 1: **Greedy versus Gradient-Based DT.** Two DTs learned on the Echocardiogram dataset. While the CART DT (left) only makes locally optimal splits, the GDT (right) performs a joint optimization of all parameters, which results in a significantly higher performance.

Example 1 The Echocardiogram dataset [11] deals with predicting one-year survival of patients after a heart attack based on tabular data from an echocardiogram. Figure 1 shows two DTs. The left tree is learned by a greedy algorithm (CART) and the right tree is learned with our gradient-based approach. We can observe that the greedy procedure leads to a suboptimal tree with a significantly lower performance. Splitting on the *wall-motion-score* is the locally optimal split (see Figure 1a), but globally, it is beneficial to split based on the *wall-motion-score* with different values conditioned on the *pericardial-effusion* in the second level (Figure 1b).

In this paper, we propose a novel approach for learning hard, axis-aligned DTs based on a joint optimization of all tree parameters with gradient descent, which we call gradient-based decision trees (GDTs). Using a gradient-based optimization, we can overcome the limitations of greedy approaches, as indicated in Figure 1b. Specifically, our contributions are:

- We introduce a dense DT representation that enables a gradient-based optimization of all tree parameters (Section 3.2).
- We present a procedure to deal with the non-differentiable nature of DTs using backpropagation with a straight-through operator (Section 3.3).
- We propose a novel tree routing that allows an efficient, parallel optimization of all tree parameters with gradient descent (Section 3.4).

We empirically evaluate GDTs on several real-world benchmark datasets (Section 4). GDTs outperform existing approaches and a greedy DT induction for binary classification tasks and achieve competitive results on multi-class datasets. On several benchmark datasets, the performance difference between GDTs and other methods is substantial. Furthermore, GDTs are less prone to overfitting. A gradient-based optimization method as used in GDTs also provides more flexibility, since splits can be adjusted during training, and custom loss functions can be easily incorporated.

2 Related Work

Greedy DT Algorithms The most prominent and still frequently used algorithms, namely CART [8] and C4.5 [34] as an extension of ID3.0 [33], date back to 1980s and both follow a greedy procedure to learn a DT. Since then, many variations to those algorithms have been proposed, for instance C5.0 [18] and GUIDE [23, 24]. However, until today, none of these algorithms was able to consistently outperform CART and C4.5 as shown for instance by Zharmagambetov et al. [40].

Lookahead DTs To overcome the issues of a greedy DT induction, many researchers focused on finding an efficient alternative. One solution to mitigate the impact of a greedy procedure are methods that look ahead during the induction [35]. However, Murthy [27] argue that those methods not only suffer from an enormous increase in computational complexity, but also suffer from pathology, i.e., they frequently produce worse trees in terms of accuracy, tree size and depth. One explanation is that lookahead trees, especially without regularization, are prone to overfitting.

Optimal DTs Optimal DTs try to optimize an objective (e.g., the purity) using approximate brute force search to find a globally optimal tree with a certain specification [40]. OCT [6] defines the optimization as a mixed integer optimization (MIO) problem which is solved using a MIO solver. DL8.5 [3] and GOSDT [21] approximate a brute force search using a branch-and-bound algorithm to remove irrelevant parts from the search space. MurTree [10] further uses dynamic programming, which reduces the runtime significantly. However, state-of-the-art approaches still require binary data and therefore a discretization of continuous features [6, 3, 10] which can lead to information loss.

Genetic DTs Another way to learn DTs in a non-greedy fashion is using evolutionary algorithms. Evolutionary algorithms perform a robust global search in the space of candidate solutions based on the concept of survival of the fittest [4]. This usually results in a better identification of feature interactions compared to a greedy, local search [12].

Oblique DTs In contrast to vanilla DTs that make hard decision at each internal node, many approaches to hierarchical mixture of expert models [16] have been proposed. They usually make soft splits, where each branch is associated with a probability [14, 13]. Further, the models do not comprise univariate, axis-aligned splits, but are oblique with respect to the axis. These adjustments to the tree architecture allow the application of further optimization algorithms, including gradient descent [14, 13]. Blanquero et al. [7] try to increase the interpretability of oblique trees by optimizing

for sparsity using fewer variables at each split and simultaneously fewer splits in the whole tree. Tanno et al. [36] combine the benefits of neural networks and DTs using so-called adaptive neural trees (ANTs) allowing a gradient-based end-to-end optimization. They employ a stochastic routing based on a Bernoulli distribution where the mean is a learned parameter. Furthermore, ANTs utilize non-linear transformer modules at the edges, making the resulting trees oblique. Norouzi et al. [28] proposed an approach for efficient non-greedy optimization of DTs that overcomes the need of soft decisions to apply gradient-based algorithms. They perform a joint optimization of all split functions and leaf parameters by minimizing a convex-concave upper bound on the tree’s empirical loss. While this allows the use of hard splits, the approach is still limited to oblique trees. Zantedeschi et al. [39] use argmin differentiation to simultaneously learn all tree parameters by relaxing a mixed-integer program for discrete parameters to allow a gradient-based optimization. This allows a deterministic tree routing which is similar to GDTs. However, they require a differentiable splitting function (e.g., a linear split function which results in oblique trees). In contrast to oblique DTs, GDTs make hard, axis-aligned splits that only consider a single feature at each split, which provides a significantly higher interpretability, especially at a split-level. This is supported by Molnar [26] where the authors argue that humans cannot comprehend explanations involving more than three dimensions at once.

Deep Neural Decision Trees (DNDTs) Yang et al. [37] propose DNDTs which realize tree models as neural networks, utilizing a soft binning function for splitting. Therefore, the resulting trees are soft, but axis-aligned, which makes this work closely related to our approach. Since the tree is generated via Kronecker product of the binning layers, the structure depends on the number of features and classes (and the number of bins). As the authors discussed, this results in poor scalability w.r.t. the number of features, which currently can only be solved by using random forests for high-dimensional datasets (> 12 features). Our approach, in contrast, scales linearly with the number of features, making it efficiently applicable for high-dimensional datasets. Furthermore, using the Kronecker product to build the tree prevents splitting on the same feature with different thresholds in the same path. For GDTs, not only the split threshold, but also the split index is a learned parameter which inherently allows splitting on the same feature multiple times.

3 Gradient-Based Axis-Aligned Decision Trees

In this section, we propose gradient-based decision trees (GDTs) as a novel approach to learn DTs. We introduce a new DT representation and a corresponding algorithm that allows learning hard, axis-aligned DTs with gradient descent. More specifically, we will use backpropagation with a straight-through (ST) operator (Section 3.3) on a dense DT representation (Section 3.2) to adjust the model parameters during the training. Furthermore, our novel tree routing (Section 3.4) allows an efficient optimization of all parameters over a complete batch with a single set of matrix operations.

3.1 Arithmetic Decision Tree Formulation

In the following, we will introduce a notation for DTs with respect to their parameters. We formulate DTs as an arithmetic function based on addition and multiplication instead of a nested concatenation of rules. This formulation is necessary for the gradient-based learning in Sections 3.2-3.4. Note that our notation and training procedure requires balanced DTs. As this is only required during training, we simply apply a basic post-hoc pruning to reduce the tree size for the application.

The parameters of a DT of depth d comprise one split threshold and one feature index for each internal node, which we denote as vectors $\boldsymbol{\tau} \in \mathbb{R}^{2^d-1}$ and $\boldsymbol{\iota} \in \mathbb{N}^{2^d-1}$ respectively, where $2^d - 1$ equals the number of internal nodes in a balanced DT. Additionally, each leaf node comprises a class membership in the case of a classification task, which we denote as the vector $\boldsymbol{\lambda} \in \mathcal{C}^{2^d}$, where \mathcal{C} is the set of classes and 2^d equals the number of leaf nodes in a balanced DT. Figure 2 shows our tree representation in comparison to a common tree representation for an exemplary DT.

Formally, we can express a DT as a function $DT(\cdot|\boldsymbol{\tau}, \boldsymbol{\iota}, \boldsymbol{\lambda}) : \mathbb{R}^n \rightarrow \mathcal{C}$ with respect to its parameters:

$$DT(\boldsymbol{x}|\boldsymbol{\tau}, \boldsymbol{\iota}, \boldsymbol{\lambda}) = \sum_{l=0}^{2^d-1} \lambda_l \mathbb{L}(\boldsymbol{x}|l, \boldsymbol{\tau}, \boldsymbol{\iota}) \quad (1)$$

Here, \mathbb{L} is a function that indicates whether a sample $\boldsymbol{x} \in \mathbb{R}^n$ belongs to a leaf l . It can be defined as a multiplication of the split functions of the preceding internal nodes.

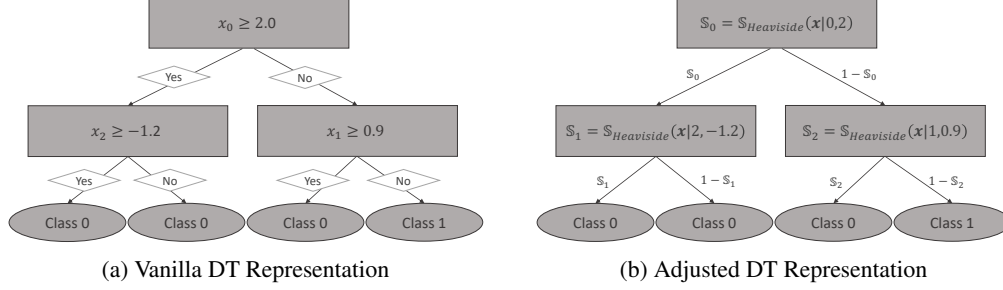


Figure 2: **DT Representations.** Exemplary DT representations with depth 2 for a dataset comprising 3 variables and 2 classes. The DT at the right can be represented using the vectors $\iota = [0, 2, 1]$, $\tau = [2.0, -1.2, 0.9]$ and $\lambda = [0, 0, 0, 1]$.

We define a split function \mathbb{S} as a Heaviside step function defined as

$$\mathbb{S}_{\text{Heaviside}}(\mathbf{x}|\iota, \tau) = \begin{cases} 1, & \text{if } x_\iota \geq \tau \\ 0, & \text{otherwise} \end{cases} \quad (2)$$

where ι is the index of the feature considered at a certain split and τ is the corresponding split threshold.

Enumerating the internal nodes of a balanced tree with depth d in a breadth-first order, we can now define the indicator function \mathbb{L} for a leaf l as follows:

$$\mathbb{L}(\mathbf{x}|l, \tau, \iota) = \prod_{j=1}^d (1 - \mathfrak{p}(l, j)) \mathbb{S}(\mathbf{x}|\tau_{i(l,j)}, \iota_{i(l,j)}) + \mathfrak{p}(l, j) (1 - \mathbb{S}(\mathbf{x}|\tau_{i(l,j)}, \iota_{i(l,j)})) \quad (3)$$

Here, i is the index of the internal node preceding a specific leaf node l at a certain depth j and can be calculated as

$$i(l, j) = 2^{j-1} + \left\lfloor \frac{l}{2^{d-(j-1)}} \right\rfloor - 1 \quad (4)$$

Further, \mathfrak{p} defines whether the left branch ($\mathfrak{p} = 0$) or the right branch ($\mathfrak{p} = 1$) was taken at the internal node preceding a leaf node l at a certain depth j . We can calculate \mathfrak{p} as

$$\mathfrak{p}(l, j) = \left\lfloor \frac{l}{2^{d-j}} \right\rfloor \bmod 2 \quad (5)$$

As becomes evident, DTs involve non-differentiable operations in terms of the split function including the split feature selection (Equation 2), which precludes the application of backpropagation for learning the parameters. More specifically, there are three challenges we need to solve if we want to use backpropagation to efficiently learn a DT:

- C1** The index ι for the split feature selection is defined as $\iota \in \mathbb{N}$. However, the index ι is a parameter of the DT and a standard optimization with gradient descent requires $\iota \in \mathbb{R}$.
- C2** The split function $\mathbb{S}(\mathbf{x}|\iota, \tau)$ is a Heaviside step function with an undefined gradient for $x_\iota = \tau$ and 0 gradient elsewhere, which precludes an efficient optimization.
- C3** The leafs in a vanilla DT comprise only the class membership as $\lambda \in \mathcal{C}$. To optimize the leaf parameters, we need $\lambda \in \mathbb{R}$ to apply gradient descent and calculate an informative loss.

The calculation of the internal node index i and path position \mathfrak{p} also involve non-differentiable operations. However, since we only focus on balanced trees, the resulting values are constant and can be calculated upfront and independent of the optimization.

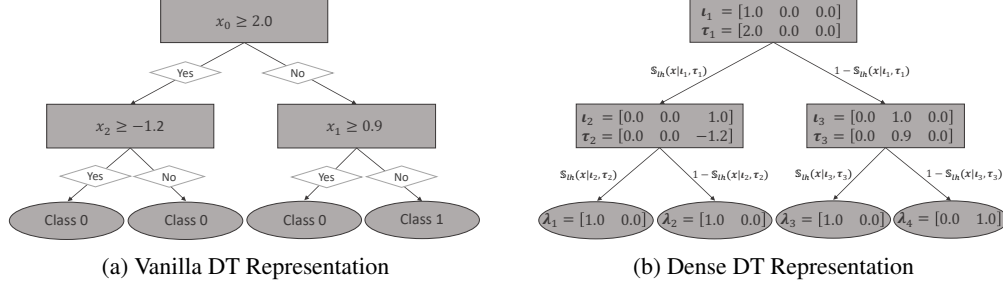


Figure 3: **Standard vs. Dense DT Representation.** Exemplary DT representations with depth 2 for a dataset comprising 3 variables and 2 classes. Here, \mathbb{S}_{lh} stands for $\mathbb{S}_{\text{logistic_hard}}$ (Equation 7).

3.2 Dense Decision Tree Representation

In this subsection, we propose a differentiable representation of the feature indices ι to allow a gradient-based optimization, which is visualized in Figure 3. Therefore, we extend the vector $\iota \in \mathbb{R}^{2^d-1}$ to a matrix $I \in \mathbb{R}^{2^d-1} \times \mathbb{R}^n$. This is achieved by one-hot encoding the feature index as $\iota \in \mathbb{R}^n$ for each internal node. This adjustment is necessary for the optimization process to account for the fact that feature indices are categorical instead of ordinal.

We further propose using a similar representation for the split thresholds as $T \in \mathbb{R}^{2^d-1} \times \mathbb{R}^n$ by storing one value for each feature as $\tau \in \mathbb{R}^n$ instead of a single value for all features. This adjustment is designed to support the optimization procedure, since the split thresholds are not interchangeable for different features: A split threshold that is reasonable for one feature might not be reasonable for another feature. By storing one split threshold for each feature, we support exploration during the optimization. This representation is inspired by the DT representation of Marton et al. [25] used for predicting a DT as a numeric output of a neural network. Further, our matrix representation for the feature selection is similar to the one proposed by Popov et al. [31] but does additionally include a matrix representation for the split thresholds.

Besides the previously mentioned advantages, using a dense DT representation allows the use of matrix multiplications for an efficient computation. Therefore, we reformulate the Heaviside split function in Equation 2 as follows:

$$\mathbb{S}_{\text{logistic}}(\mathbf{x}|\iota, \tau) = S\left(\sum_{i=0}^n \iota_i x_i - \sum_{i=0}^n \iota_i \tau_i\right) \quad (6)$$

$$\mathbb{S}_{\text{logistic_hard}}(\mathbf{x}|\iota, \tau) = \lfloor \mathbb{S}_{\text{logistic}}(\mathbf{x}|\iota, \tau) \rfloor \quad (7)$$

where $S(x) = \frac{1}{1+e^{-x}}$ is the logistic function and $\lfloor \cdot \rfloor$ stands for rounding to the closest integer. For our case, where ι is one-hot encoded, $\mathbb{S}_{\text{logistic_hard}}(\mathbf{x}|\iota, \tau) = \mathbb{S}_{\text{Heaviside}}(\mathbf{x}|\iota, \tau)$ holds.

3.3 Backpropagation of Decision Tree Loss

While the dense DT representation introduced in the previous section emphasizes an efficient learning of axis-aligned DTs, it does not solve **C1-C3**. Therefore, in this subsection, we will explain how we solve those challenges by using a ST operator during backpropagation.

For the function value calculation in the forward pass, we need to assure that ι is a one-hot encoded vector. This can be achieved by applying a hardmax function on the feature index vector for each internal node. However, applying a hardmax is a non-differentiable operation, which precludes gradient computation. To overcome this issue, we use the ST operator [5]: For the forward pass, we apply the hardmax as is. For the backward pass, however, we exclude this operation and directly propagate back the gradients of ι . Accordingly, we can optimize the parameters of ι where $\iota \in \mathbb{R}$ while still using axis-aligned splits during training (**C1**). However, this procedure introduces a mismatch between the forward and backward pass. To reduce this mismatch, we additionally perform an entmax transformation [30] to generate a sparse distribution over ι before applying the hardmax.

Similarly, we use the ST operator to assure hard splits (Equation 7) by excluding $\lfloor \cdot \rfloor$ for the backward pass (C2). Using the sigmoid logistic function before applying the ST operator (see Equation 6) utilizes the distance to the split threshold as additional information for the gradient calculation. If the feature considered at an internal node is close to the split threshold for a specific sample, this will result in smaller gradients compared to a sample that is more distant.

Furthermore, we need to adjust the leaf nodes of the DT to allow an efficient loss calculation (C3). Vanilla DTs comprise the predicted class for each leaf node and are functions $DT : \mathbb{R}^n \rightarrow \mathcal{C}$. We use a probability distribution at each leaf node and therefore define DTs as a function $DT : \mathbb{R}^n \rightarrow \mathbb{R}^c$ where c is the number of classes. Accordingly, the parameters of the leaf nodes are defined as $L \in \mathbb{R}^{2^n} \times \mathbb{R}^c$ for the whole tree and $\lambda \in \mathbb{R}^c$ for a specific leaf node. This adjustment allows the application of standard loss functions. For classification tasks, we use a cross-entropy loss including a focal factor [22] (see Appendix D for further details).

3.4 Deterministic Tree Routing and Training Procedure

In the previous subsections, we introduced the adjustments that are necessary to apply gradient descent to decision trees. During the optimization, we calculate the gradients with backpropagation implemented using automatic differentiation based on the computation graph of the tree pass function. The tree pass function to calculate the function values is summarized in Algorithm 1 and utilizes the adjustments introduced in the previous sections. Our tree routing allows calculating the tree pass function over a complete batch as a single set of matrix operations, which allows an efficient computation. We also want to note that our dense representation can be converted into an equivalent vanilla DT representation at each point in time. Similarly, the balanced nature of GDTs is only required during the gradient-based optimization and standard pruning techniques to reduce the tree size are applied post-hoc.

Furthermore, our implementation optimizes the gradient descent algorithm by exploiting common stochastic gradient descent techniques, including mini-batch calculation and momentum using the Adam optimizer [17] with weight averaging [15] (further details can be found in the Appendix A). Moreover, we implement early stopping and random restarts to avoid bad initial parametrizations, where the best parameters are selected based on the validation loss.

Algorithm 1 Tree Pass Function

```

1: function PASS( $I, T, L, \mathbf{x}$ )
2:    $I \leftarrow \text{entmax}(I)$  ▷ ST operator
3:    $c_1^* \leftarrow I_i - \text{hardmax}(I_i)$ 
4:    $I \leftarrow I - c_1^*$ 
5:    $\hat{\mathbf{y}} \leftarrow [0]^c$ 
6:   for  $l = 0, \dots, 2^d - 1$  do
7:      $p \leftarrow 1$ 
8:     for  $j = 1, \dots, d$  do
9:        $i \leftarrow 2^{j-1} + \lfloor \frac{l}{2^{d-(j-1)}} \rfloor - 1$  ▷ Equation 4
10:       $p \leftarrow \lfloor \frac{l}{2^{d-j}} \rfloor \bmod 2$  ▷ Equation 5
11:       $s \leftarrow S \left( \sum_{i=0}^n T_{i,i} I_{i,i} - \sum_{i=0}^n x_i I_{i,i} \right)$  ▷ Equation 6
12:       $c_2^* = s - \lfloor s \rfloor$  ▷ ST operator
13:       $s \leftarrow s - c_2^*$ 
14:       $p \leftarrow p \left( (1 - p) s + p (1 - s) \right)$  ▷ Equation 3
15:    end for
16:     $\hat{\mathbf{y}} \leftarrow \hat{\mathbf{y}} + L_l p$  ▷ Equation 1
17:  end for
18:  return  $\sigma(\hat{\mathbf{y}})$  ▷ Apply softmax function  $\sigma$  to get predicted probability distribution
19: end function

```

4 Experimental Evaluation

The following experiments aim to evaluate the predictive capability of GDTs against existing methods.

4.1 Experimental Setup

Datasets and Preprocessing The experiments were conducted on several benchmark datasets, mainly from the UCI Machine Learning repository [11]. For all datasets, we performed a standard preprocessing: We applied leave-one-out encoding to all categorical features. Similar to Popov et al. [31], we further perform a quantile transform, making each feature follow a normal distribution. We use a random 80%/20% train-test split for all datasets. To account for class imbalance, we rebalanced datasets using SMOTE [9] if the minority class accounts for less than $\frac{25}{c-1}\%$ of the data points, where c is the number of classes. For GDTs and DNDTs we use 20% of the training data as validation data for early stopping. As DL8.5 requires binary features, we discretized all numeric features using quantile binning with 5 bins and one-hot encoded all categorical features. Further information on the datasets along with the data sources can be found in the Appendix B.

Methods We focus on hard, axis-aligned DTs and compare GDTs to the following methods:

- **CART**: We use the sklearn [29] implementation, which uses an optimized version of the CART algorithm. While CART usually only uses Gini as impurity measure, we also allow information gain/entropy as an option during our hyperparameter optimization. Since this is also the relevant difference between CART and C4.5, we decided to only use optimized CART, which is also the stronger benchmark.
- **Evolutionary DTs**: We use GeneticTree [32] which implements an efficient learning of DTs with a genetic algorithm.
- **DNDT** [37]: We use the official DNDT implementation [38]. For a fair comparison, we enforce binary trees by setting the number of cut points to 1. Furthermore, since DNDTs are soft during the training, we enforced hard splits during inference to ensure comparability. Due to scalability issues, DNDTs were only applied to datasets with a maximum of 12 features, as suggested by Yang et al. [37].
- **DL8.5** [3]: We use the official DL8.5 implementation [2] for learning optimal DTs including improvements from MurTree [10] which reduces the runtime significantly.

GDTs are implemented in Python using TensorFlow [1]¹. For GDTs, we further applied a simple post-hoc pruning to remove all branches with zero samples based on one pass of the training data.

Hyperparameter Optimization To select the optimal hyperparameters, we conducted a random search with cross-validation. The complete list of relevant hyperparameters for each approach along with additional details on the selection can be found in the Appendix D.

4.2 Results

GDTs are competitive to existing DT learners First, we evaluated the performance of GDTs against existing approaches on the benchmark datasets in terms of the macro F1-Score, which also accounts for class imbalance (Table 1). We note the mean and mean reciprocal rank (MRR), similar to Yang et al. [37]. Overall, GDTs outperformed existing approaches for binary classification tasks (best MRR of 0.771) and achieved competitive results for multi-class tasks (second-best MRR of 0.619). More specifically, GDTs outperformed state-of-the-art non-greedy DT approaches for both, binary and multi-class tasks. In addition, GDTs outperformed DNDTs on 12 out of 16 datasets, making it the substantially better gradient-based approach. For binary classification tasks, GDTs demonstrated superior performance over CART, achieving the best performance on 13 datasets as compared to only 6 datasets for CART. Notably, the performance difference between GDTs and existing methods was substantial for several datasets, as for instance on *Echocardiogram*, *Heart Disease* and *Absenteeism*.

For multi-class datasets, GDTs only achieved the second-best overall performance. Especially for high-dimensional datasets with a high number of classes, CART achieved the highest performance.

¹The code of our implementation is available under <https://github.com/s-marton/GradientBasedDecisionTrees>.

Table 1: **Performance Comparison.** We report macro F1-scores (mean \pm stdev over 10 trials). We also report the rank of each approach in brackets. The datasets are sorted by the number of features. The top part comprises binary classification tasks and the bottom part multi-class datasets.

	Gradient-Based		Non-Greedy		Greedy
	GDT (ours)	DNDT	GeneticTree	DL8.5	CART
Blood Transfusion	0.628 \pm 0.036 (1)	0.543 \pm 0.051 (5)	0.575 \pm 0.094 (4)	0.590 \pm 0.034 (3)	0.613 \pm 0.044 (2)
Banknote Authentication	0.987 \pm 0.007 (1)	0.888 \pm 0.013 (5)	0.922 \pm 0.021 (4)	0.962 \pm 0.011 (3)	0.982 \pm 0.007 (2)
Titanic	0.776 \pm 0.025 (1)	0.726 \pm 0.049 (5)	0.730 \pm 0.074 (4)	0.754 \pm 0.031 (2)	0.738 \pm 0.057 (3)
Raisins	0.840 \pm 0.022 (4)	0.821 \pm 0.033 (5)	0.857 \pm 0.021 (1)	0.849 \pm 0.027 (3)	0.852 \pm 0.017 (2)
Rice	0.926 \pm 0.007 (3)	0.919 \pm 0.012 (5)	0.927 \pm 0.005 (2)	0.925 \pm 0.008 (4)	0.927 \pm 0.006 (1)
Echocardiogram	0.658 \pm 0.113 (1)	0.622 \pm 0.114 (3)	0.628 \pm 0.105 (2)	0.609 \pm 0.112 (4)	0.555 \pm 0.111 (5)
Wisconsin Breast Cancer	0.904 \pm 0.022 (2)	0.913 \pm 0.032 (1)	0.892 \pm 0.028 (4)	0.896 \pm 0.021 (3)	0.886 \pm 0.025 (5)
Loan House	0.714 \pm 0.041 (1)	0.694 \pm 0.036 (2)	0.451 \pm 0.086 (5)	0.607 \pm 0.045 (4)	0.662 \pm 0.034 (3)
Heart Failure	0.750 \pm 0.070 (3)	0.754 \pm 0.062 (2)	0.748 \pm 0.068 (4)	0.692 \pm 0.062 (5)	0.775 \pm 0.054 (1)
Heart Disease	0.779 \pm 0.047 (1)	$n > 12$	0.704 \pm 0.059 (4)	0.722 \pm 0.065 (2)	0.715 \pm 0.062 (3)
Adult	0.743 \pm 0.034 (2)	$n > 12$	0.464 \pm 0.055 (4)	0.723 \pm 0.011 (3)	0.771 \pm 0.011 (1)
Bank Marketing	0.640 \pm 0.027 (1)	$n > 12$	0.473 \pm 0.002 (4)	0.502 \pm 0.011 (3)	0.608 \pm 0.018 (2)
Congressional Voting	0.950 \pm 0.021 (1)	$n > 12$	0.942 \pm 0.021 (2)	0.924 \pm 0.043 (4)	0.933 \pm 0.032 (3)
Absenteeism	0.626 \pm 0.047 (1)	$n > 12$	0.432 \pm 0.073 (4)	0.587 \pm 0.047 (2)	0.564 \pm 0.042 (3)
Hepatitis	0.608 \pm 0.078 (2)	$n > 12$	0.446 \pm 0.024 (4)	0.586 \pm 0.083 (3)	0.622 \pm 0.078 (1)
German	0.592 \pm 0.068 (1)	$n > 12$	0.412 \pm 0.006 (4)	0.556 \pm 0.035 (3)	0.589 \pm 0.065 (2)
Mushroom	1.000 \pm 0.001 (1)	$n > 12$	0.984 \pm 0.003 (4)	0.999 \pm 0.001 (2)	0.999 \pm 0.001 (3)
Credit Card	0.674 \pm 0.014 (4)	$n > 12$	0.685 \pm 0.004 (1)	0.679 \pm 0.007 (3)	0.683 \pm 0.010 (2)
Horse Colic	0.842 \pm 0.039 (1)	$n > 12$	0.496 \pm 0.169 (4)	0.708 \pm 0.038 (3)	0.786 \pm 0.062 (2)
Thyroid	0.905 \pm 0.010 (2)	$n > 12$	0.605 \pm 0.116 (4)	0.682 \pm 0.018 (3)	0.922 \pm 0.011 (1)
Cervical Cancer	0.521 \pm 0.043 (1)	$n > 12$	0.514 \pm 0.034 (2)	0.488 \pm 0.027 (4)	0.506 \pm 0.034 (3)
Spambase	0.903 \pm 0.025 (2)	$n > 12$	0.863 \pm 0.019 (3)	0.863 \pm 0.011 (4)	0.917 \pm 0.011 (1)
Mean	0.771 \pm 0.142 (1)	-	0.671 \pm 0.196 (4)	0.723 \pm 0.154 (3)	0.755 \pm 0.154 (2)
Mean Reciprocal Rank	0.758 \pm 0.306 (1)	0.370 \pm 0.268 (3)	0.365 \pm 0.228 (4)	0.335 \pm 0.090 (5)	0.556 \pm 0.293 (2)
Iris	0.938 \pm 0.057 (1)	0.870 \pm 0.063 (5)	0.912 \pm 0.055 (3)	0.909 \pm 0.046 (4)	0.937 \pm 0.046 (2)
Balance Scale	0.593 \pm 0.045 (1)	0.475 \pm 0.104 (5)	0.529 \pm 0.043 (3)	0.525 \pm 0.039 (4)	0.574 \pm 0.030 (2)
Car	0.440 \pm 0.085 (3)	0.485 \pm 0.064 (2)	0.306 \pm 0.068 (4)	0.273 \pm 0.063 (5)	0.489 \pm 0.094 (1)
Glass	0.560 \pm 0.090 (3)	0.434 \pm 0.072 (5)	0.586 \pm 0.090 (2)	0.501 \pm 0.100 (4)	0.663 \pm 0.086 (1)
Contraceptive	0.496 \pm 0.050 (1)	0.364 \pm 0.050 (3)	0.290 \pm 0.048 (5)	0.292 \pm 0.036 (4)	0.384 \pm 0.075 (2)
Solar Flare	0.151 \pm 0.033 (3)	0.171 \pm 0.051 (1)	0.146 \pm 0.018 (4)	0.144 \pm 0.034 (5)	0.157 \pm 0.022 (2)
Wine	0.933 \pm 0.031 (1)	0.858 \pm 0.041 (4)	0.888 \pm 0.039 (3)	0.852 \pm 0.022 (5)	0.907 \pm 0.042 (2)
Zoo	0.874 \pm 0.111 (3)	$n > 12$	0.782 \pm 0.111 (4)	0.911 \pm 0.106 (2)	0.943 \pm 0.076 (1)
Lymphography	0.610 \pm 0.191 (1)	$n > 12$	0.381 \pm 0.124 (4)	0.574 \pm 0.196 (2)	0.548 \pm 0.154 (3)
Segment	0.941 \pm 0.009 (2)	$n > 12$	0.715 \pm 0.114 (4)	0.808 \pm 0.013 (3)	0.963 \pm 0.010 (1)
Dermatology	0.930 \pm 0.030 (2)	$n > 12$	0.785 \pm 0.126 (4)	0.885 \pm 0.036 (3)	0.957 \pm 0.026 (1)
Landsat	0.807 \pm 0.011 (2)	$n > 12$	0.628 \pm 0.084 (4)	0.783 \pm 0.008 (3)	0.835 \pm 0.011 (1)
Annealing	0.638 \pm 0.126 (3)	$n > 12$	0.218 \pm 0.053 (4)	0.787 \pm 0.121 (2)	0.866 \pm 0.094 (1)
Splice	0.873 \pm 0.030 (2)	$n > 12$	0.486 \pm 0.157 (3)	> 60 min	0.881 \pm 0.021 (1)
Mean	0.699 \pm 0.240 (2)	-	0.547 \pm 0.252(4)	0.634 \pm 0.268(3)	0.722 \pm 0.255 (1)
Mean Reciprocal Rank	0.619 \pm 0.303 (2)	0.383 \pm 0.293 (3)	0.288 \pm 0.075 (5)	0.315 \pm 0.116 (4)	0.774 \pm 0.274 (1)

This result can be explained by the dense DT representation required for the gradient-based optimization. Using our representation, the difficulty of the optimization task increases with the number of features (more parameters at each internal node) and the number of classes (more parameters at each leaf node). Therefore, in future work, we aim to optimize the proposed dense representation, e.g., by using parameter sharing techniques.

GTDs have a small effective tree size The effective tree size (= size of the tree after pruning) of GTDs is smaller than CART for binary and slightly larger for multi-class tasks (see Table 2). Only the tree size for GeneticTree is significantly smaller, which is caused by the complexity penalty of the genetic algorithm. DL8.5 also has a smaller average tree size than CART and GDT. We can explain the comparatively small average tree sizes by the fact that DL8.5 was only feasible up to a depth of 4 (maximum of 31 total nodes) due to the high computational complexity. The tree size for DNDTs scales with the number of features (and classes) which quickly results in large trees. Furthermore, pruning DNDTs is non-trivial due to the use of the Kronecker product (it is not sufficient to prune subtrees bottom-up), which is why we did not apply pruning for DNDTs.

GDTs are robust to overfitting We can observe that gradient-based approaches were more robust and less prone to overfitting than a greedy optimization with CART and alternative non-greedy approaches. We measure overfitting by the difference between the mean train and test performance (see Table 2). GDTs have a difference between the train and test performance of 0.051 for binary tasks, which is significantly smaller than CART (0.183), GeneticTree (0.204) and DL8.5 (0.202). DNDTs,

Table 2: **Summarized Results.** Left: Tree size after HPO. Mid: Difference between train and test performance as overfitting indicator. Right: Impact of HPO by measuring the performance difference with and without HPO. The complete results for each dataset are listed in the Appendix C.

	Tree Size		Train-Test Difference		HPO Impact	
	binary	multi-class	binary	multi-class	binary	multi-class
GDT	54.2	86.2	0.051	0.174	0.007	0.036
DNDT	886.7	906.9	0.039	0.239	0.051	0.000
GeneticTree	6.9	20.2	0.204	0.258	-0.001	-0.018
DL8.5	27.5	28.9	0.202	0.260	-	-
CART	66.7	76.0	0.183	0.247	0.007	-0.016

which are also gradient-based, achieved an even smaller difference of 0.039. For multi-class tasks, the difference was significantly smaller for GDTs compared to any other approach. For DL8.5, we can observe very strong overfitting (second-highest difference for binary and highest for multi-class tasks) which can also explain why optimal DTs did not achieve superior results on test data. These findings are similar to those reported by Zharmagambetov et al. [40].

GDTs do not rely on extensive hyperparameter optimization An advantage of DTs over more sophisticated models, besides their interpretability, is that greedy approaches do not rely on extensive hyperparameter optimization (HPO) to achieve good results. In this experiment, we show that the same is true for GDTs. We evaluated the performance of the approaches with their default configuration and compared it with the performance after HPO (see Table 2). Overall, the impact of HPO was rather small for all approaches. For multi-class tasks, HPO even resulted in a decrease of the average test performance for CART and GeneticTree. This observation can be explained by the strong overfitting of those approaches, which makes estimating the test performance difficult, even when using cross-validation. Thus, suboptimal parameters can be selected based on the validation performance, resulting in a decrease of the average test performance. Furthermore, when using the default parameters, GDTs still outperform on binary tasks (highest MRR and most wins) and achieve competitive results for multi-class tasks (second-highest MRR and second-most wins). Detailed results with default parameters for all datasets are listed in the Appendix C.

GDTs can be learned efficiently for large and high-dimensional datasets Greedy optimization with CART was significantly faster than any other approach (less than a second) for each dataset. Nevertheless, for most datasets, learning a GDT took less than 30 seconds (mean runtime of 35 seconds). DNDT achieved similar runtimes to GDT. DL8.5 had a low runtime < 10 seconds for most datasets. However we can observe scalability issues with the number of features and number of samples, as DL8.5 had a significantly higher runtime than GDT for several datasets (e.g., ~ 300 seconds for *Credit Card* and > 830 seconds for *Landsat*). For *Splice*, DL8.5 did not converge after 60 minutes and the optimization was terminated. The complete runtimes for each approach are listed in the Appendix C.

5 Conclusion and Future Work

In this paper, we proposed a novel method for learning hard, axis-aligned DTs based on a joint optimization of all tree parameters with gradient descent. We use backpropagation with a ST operator to deal with the non-differentiable nature of DTs. We further introduced a dense DT representation and a novel tree pass function which allows an efficient optimization. Using a gradient-based optimization, GDTs are not prone to locally optimal solutions, as it is the case for standard, greedy DT induction methods like CART. We empirically showed that GDTs outperformed existing approaches on binary classification tasks and achieved competitive results on multi-class tasks. The performance increase when using our approach was substantial for several datasets, which makes GDTs an important extension to existing approaches for DT learning. Moreover, GDTs significantly outperformed DNDTs as gradient-based benchmark.

Furthermore, a gradient-based optimization provides more flexibility. It is straightforward to use a custom loss function that is well-suited for the specific application scenario. Another advantage is the

possibility to relearn the threshold value as well as the split index. This makes GDTs suitable for dynamic environments, as for instance online learning tasks.

Currently, GDTs use a standard post-hoc pruning. In future work, we want to consider pruning already during the training, for instance through a learnable choice parameter to decide if a node is pruned, similar to Zantedeschi et al. [39]. While we focused on stand-alone DTs to generate intrinsically interpretable models, GDTs can be extended to ensembles as a performance-interpretability trade-off, which is subject to future work.

References

- [1] Martín Abadi, Ashish Agarwal, Paul Barham, Eugene Brevdo, Zhifeng Chen, Craig Citro, Greg S. Corrado, Andy Davis, Jeffrey Dean, Matthieu Devin, Sanjay Ghemawat, Ian Goodfellow, Andrew Harp, Geoffrey Irving, Michael Isard, Yangqing Jia, Rafal Jozefowicz, Lukasz Kaiser, Manjunath Kudlur, Josh Levenberg, Dandelion Mané, Rajat Monga, Sherry Moore, Derek Murray, Chris Olah, Mike Schuster, Jonathon Shlens, Benoit Steiner, Ilya Sutskever, Kunal Talwar, Paul Tucker, Vincent Vanhoucke, Vijay Vasudevan, Fernanda Viégas, Oriol Vinyals, Pete Warden, Martin Wattenberg, Martin Wicke, Yuan Yu, and Xiaoqiang Zheng. TensorFlow: Large-scale machine learning on heterogeneous systems, 2015. URL <https://www.tensorflow.org/>. Software available from tensorflow.org.
- [2] G. Aglin, S. Nijssen, and P. Schaus. Pydl8.5. <https://github.com/aia-uclouvain/pydl8.5>, 2022. Accessed 13.11.2022.
- [3] Gaël Aglin, Siegfried Nijssen, and Pierre Schaus. Learning optimal decision trees using caching branch-and-bound search. In *Proceedings of the AAAI Conference on Artificial Intelligence*, volume 34, pages 3146–3153, 2020.
- [4] Rodrigo Coelho Barros, Márcio Porto Basgalupp, Andre CPLF De Carvalho, and Alex A Freitas. A survey of evolutionary algorithms for decision-tree induction. *IEEE Transactions on Systems, Man, and Cybernetics, Part C (Applications and Reviews)*, 42(3):291–312, 2011.
- [5] Yoshua Bengio, Nicholas Léonard, and Aaron Courville. Estimating or propagating gradients through stochastic neurons for conditional computation. *arXiv preprint arXiv:1308.3432*, 2013.
- [6] Dimitris Bertsimas and Jack Dunn. Optimal classification trees. *Machine Learning*, 106(7): 1039–1082, 2017.
- [7] Rafael Blanquero, Emilio Carrizosa, Cristina Molero-Río, and Dolores Romero Morales. Sparsity in optimal randomized classification trees. *European Journal of Operational Research*, 284(1):255–272, 2020.
- [8] Leo Breiman, J. H. Friedman, R. A. Olshen, and C. J. Stone. *Classification and Regression Trees*. Wadsworth, 1984. ISBN 0-534-98053-8. URL <http://lyle.smu.edu/~mhd/8331f06/cart.pdf>.
- [9] Nitesh V Chawla, Kevin W Bowyer, Lawrence O Hall, and W Philip Kegelmeyer. Smote: synthetic minority over-sampling technique. *Journal of artificial intelligence research*, 16: 321–357, 2002.
- [10] Emir Demirović, Anna Lukina, Emmanuel Hebrard, Jeffrey Chan, James Bailey, Christopher Leckie, Kotagiri Ramamohanarao, and Peter J Stuckey. Murtree: Optimal decision trees via dynamic programming and search. *Journal of Machine Learning Research*, 23(26):1–47, 2022.
- [11] Dheeru Dua and Casey Graff. UCI machine learning repository, 2017. URL <http://archive.ics.uci.edu/ml>.
- [12] Alex A Freitas. *Data mining and knowledge discovery with evolutionary algorithms*. Springer Science & Business Media, 2002.
- [13] Nicholas Frosst and Geoffrey Hinton. Distilling a neural network into a soft decision tree. *arXiv preprint arXiv:1711.09784*, 2017.

- [14] Ozan Irsoy, Olcay Taner Yıldız, and Ethem Alpaydın. Soft decision trees. In *Proceedings of the 21st international conference on pattern recognition (ICPR2012)*, pages 1819–1822. IEEE, 2012.
- [15] Pavel Izmailov, Dmitrii Podoprikin, Timur Garipov, Dmitry Vetrov, and Andrew Gordon Wilson. Averaging weights leads to wider optima and better generalization. *arXiv preprint arXiv:1803.05407*, 2018.
- [16] Michael I Jordan and Robert A Jacobs. Hierarchical mixtures of experts and the em algorithm. *Neural computation*, 6(2):181–214, 1994.
- [17] Diederik P Kingma and Jimmy Ba. Adam: A method for stochastic optimization. *arXiv preprint arXiv:1412.6980*, 2014.
- [18] Max Kuhn, Kjell Johnson, et al. *Applied predictive modeling*, volume 26. Springer, 2013.
- [19] Hyafil Laurent and Ronald L Rivest. Constructing optimal binary decision trees is np-complete. *Information processing letters*, 5(1):15–17, 1976.
- [20] Zhaoqi Leng, Mingxing Tan, Chenxi Liu, Ekin Dogus Cubuk, Xiaojie Shi, Shuyang Cheng, and Dragomir Anguelov. Polyloss: A polynomial expansion perspective of classification loss functions. *arXiv preprint arXiv:2204.12511*, 2022.
- [21] Jimmy Lin, Chudi Zhong, Diane Hu, Cynthia Rudin, and Margo Seltzer. Generalized and scalable optimal sparse decision trees. In *International Conference on Machine Learning*, pages 6150–6160. PMLR, 2020.
- [22] Tsung-Yi Lin, Priya Goyal, Ross Girshick, Kaiming He, and Piotr Dollár. Focal loss for dense object detection. In *Proceedings of the IEEE international conference on computer vision*, pages 2980–2988, 2017.
- [23] Wei-Yin Loh. Regression trees with unbiased variable selection and interaction detection. *Statistica sinica*, pages 361–386, 2002.
- [24] Wei-Yin Loh. Improving the precision of classification trees. *The Annals of Applied Statistics*, pages 1710–1737, 2009.
- [25] Sascha Marton, Stefan Lüdtke, Christian Bartelt, Andrej Tschalzev, and Heiner Stuckenschmidt. Explaining neural networks without access to training data. *arXiv preprint arXiv:2206.04891*, 2022.
- [26] Christoph Molnar. *Interpretable machine learning*. Lulu. com, 2020.
- [27] Kolluru Venkata Sreerama Murthy. *On growing better decision trees from data*. The Johns Hopkins University, 1996.
- [28] Mohammad Norouzi, Maxwell Collins, Matthew A Johnson, David J Fleet, and Pushmeet Kohli. Efficient non-greedy optimization of decision trees. *Advances in neural information processing systems*, 28, 2015.
- [29] F. Pedregosa, G. Varoquaux, A. Gramfort, V. Michel, B. Thirion, O. Grisel, M. Blondel, P. Prettenhofer, R. Weiss, V. Dubourg, J. Vanderplas, A. Passos, D. Cournapeau, M. Brucher, M. Perrot, and E. Duchesnay. Scikit-learn: Machine learning in Python. *Journal of Machine Learning Research*, 12:2825–2830, 2011.
- [30] Ben Peters, Vlad Niculae, and André FT Martins. Sparse sequence-to-sequence models. *arXiv preprint arXiv:1905.05702*, 2019.
- [31] Sergei Popov, Stanislav Morozov, and Artem Babenko. Neural oblivious decision ensembles for deep learning on tabular data. *arXiv preprint arXiv:1909.06312*, 2019.
- [32] Karol Pysiak. Genetictree. <https://github.com/pysiakk/GeneticTree>, 2021. Accessed 17.08.2022.
- [33] J. Ross Quinlan. Induction of decision trees. *Machine learning*, 1(1):81–106, 1986.

- [34] J. Ross Quinlan. *C4.5: programs for machine learning*. Morgan Kaufmann Publishers Inc., San Francisco, CA, USA, 1993. ISBN 1-55860-238-0. URL <http://portal.acm.org/citation.cfm?id=152181>.
- [35] UK Sarkar, PP Chakrabarti, Sujoy Ghose, and SC DeSarkar. Improving greedy algorithms by lookahead-search. *Journal of Algorithms*, 16(1):1–23, 1994.
- [36] Ryutaro Tanno, Kai Arulkumaran, Daniel Alexander, Antonio Criminisi, and Aditya Nori. Adaptive neural trees. In *International Conference on Machine Learning*, pages 6166–6175. PMLR, 2019.
- [37] Yongxin Yang, Irene Garcia Morillo, and Timothy M Hospedales. Deep neural decision trees. *arXiv preprint arXiv:1806.06988*, 2018.
- [38] Yongxin Yang, Irene Garcia Morillo, and Timothy M. Hospedales. Deep neural decision trees. <https://github.com/w00L/DNDT>, 2022. Accessed 13.11.2022.
- [39] Valentina Zantedeschi, Matt Kusner, and Vlad Niculae. Learning binary decision trees by argmin differentiation. In *International Conference on Machine Learning*, pages 12298–12309. PMLR, 2021.
- [40] Arman Zharmagambetov, Suryabhan Singh Hada, Magzhan Gabidolla, and Miguel A Carreira-Perpinán. Non-greedy algorithms for decision tree optimization: An experimental comparison. In *2021 International Joint Conference on Neural Networks (IJCNN)*, pages 1–8. IEEE, 2021.

A Gradient Descent Optimization

We use stochastic gradient descent (SGD) to minimize the loss function of GDTs, which is outlined in Algorithm 2. We use backpropagation to calculate the gradients in Line 11-13. Furthermore, our implementation optimizes Algorithm 2 by exploiting common SGD techniques, including mini-batch calculation and momentum using the Adam optimizer [17]. We further apply weight averaging [15] over 5 consecutive checkpoints, similar to Popov et al. [31]. Our novel tree pass function allows formulating Line 7-9 as a single matrix operation for a complete batch, which results in a very efficient optimization. Moreover, we implement an early stopping procedure. To avoid bad initial parametrizations during the initialization, we additionally implement random restarts where the best parameters are selected based on the validation loss.

Algorithm 2 Gradient Descent Training for Decision Trees

```

1: function TRAINDT( $I, T, L, X, \mathbf{y}, n, c, d, \xi$ )
2:    $I \sim \mathcal{U}\left(-\sqrt{\frac{6}{2^{2d-1}+n}}, \sqrt{\frac{6}{2^{2d-1}+n}}\right)$ 
3:    $T \sim \mathcal{U}\left(-\sqrt{\frac{6}{2^{2d-1}+n}}, \sqrt{\frac{6}{2^{2d-1}+n}}\right)$ 
4:    $L \sim \mathcal{U}\left(-\sqrt{\frac{6}{2^{2d}+c}}, \sqrt{\frac{6}{2^{2d}+c}}\right)$ 
5:   for  $i = 1, \dots, \xi$  do
6:      $\hat{\mathbf{y}} \leftarrow \emptyset$ 
7:     for  $j = 1, \dots, |X|$  do
8:        $\hat{y}_j = \text{PASS}(I, T, L, X_j)$ 
9:        $\hat{\mathbf{y}} \leftarrow \hat{\mathbf{y}} \cup \hat{y}_j$ 
10:    end for
11:     $I \leftarrow I + \eta \frac{\partial}{\partial I} \mathcal{L}(\mathbf{y}, \hat{\mathbf{y}})$  ▷ Calculate gradients with backpropagation
12:     $T \leftarrow T + \eta \frac{\partial}{\partial T} \mathcal{L}(\mathbf{y}, \hat{\mathbf{y}})$  ▷ Calculate gradients with backpropagation
13:     $L \leftarrow L + \eta \frac{\partial}{\partial L} \mathcal{L}(\mathbf{y}, \hat{\mathbf{y}})$  ▷ Calculate gradients with backpropagation
14:  end for
15: end function

```

B Datasets

The datasets along with their specifications and source are summarized in Table 3. For all datasets, we performed a standard preprocessing: We applied Leave-one-out encoding to all categorical features. Similar to Popov et al. [31], we further perform a quantile transform, making each feature follows a normal distribution. We use a random 80%/20% train-test split for all datasets. To account for class imbalance, we rebalanced datasets using SMOTE [9] when the minority class accounts for less than $\frac{25}{c-1}\%$ of the data points, where c is the number of classes. Since GDTs and DNDTs requires a validation set for early stopping, we performed another 80%/20% split on the training data for those approaches. For DL8.5 additional preprocessing was necessary since they can only handle binary features. Therefore, we one-hot encoded all categorical features and discretized numeric features by one-hot encoding them using quantile binning with 5 bins.

Table 3: Dataset Specifications.

Dataset Name	Number of Features	Number of Samples	Samples by Class	Number of Classes	Link
Blood Transfusion	4	748	178 / 570	2	https://archive.ics.uci.edu/ml/datasets/Blood+Transfusion+Service+Center
Banknote Authentication	4	1372	610 / 762	2	https://archive.ics.uci.edu/ml/datasets/banknote+authentication
Titanic	7	891	342 / 549	2	https://www.kaggle.com/c/titanic
Raisin	7	900	450 / 450	2	https://archive.ics.uci.edu/ml/datasets/Raisin+Dataset
Rice	7	3810	1630 / 2180	2	https://archive.ics.uci.edu/ml/datasets/Rice+%28Cammeo+and+Osmancik%29
Echocardiogram	8	132	107 / 25	2	https://archive.ics.uci.edu/ml/datasets/echocardiogram
Wisconsin Diagnostic Breast Cancer	10	569	212 / 357	2	https://archive.ics.uci.edu/ml/datasets/breast+cancer+wisconsin+(diagnostic)
Loan House	11	614	422 / 192	2	https://www.kaggle.com/code/sazid28/home-loan-prediction/data
Heart Failure	12	299	96 / 203	2	https://archive.ics.uci.edu/ml/datasets/Heart+failure+clinical+records
Heart Disease	13	303	164 / 139	2	https://archive.ics.uci.edu/ml/datasets/heart+disease
Adult	14	32561	7841 / 24720	2	https://archive.ics.uci.edu/ml/datasets/adult
Bank Marketing	14	45211	5289 / 39922	2	https://archive.ics.uci.edu/ml/datasets/bank+marketing
Congressional Voting	16	435	267 / 168	2	https://archive.ics.uci.edu/ml/datasets/congressional+voting+records
Absenteeism	18	740	279 / 461	2	https://archive.ics.uci.edu/ml/datasets/Absenteeism+at+work
Hepatitis	19	155	32 / 123	2	https://archive.ics.uci.edu/ml/datasets/hepatitis
German	20	1000	300 / 700	2	https://archive.ics.uci.edu/ml/datasets/statlog+(german+credit+data)
Mushrooms	22	8124	4208 / 3916	2	https://archive.ics.uci.edu/ml/datasets/mushroom
Credit Card	23	30000	23364 / 6636	2	https://archive.ics.uci.edu/ml/datasets/default+of+credit+card+clients
Horse Colic	26	368	232 / 136	2	https://archive.ics.uci.edu/ml/datasets/Horse+Colic
Thyroid	29	9172	2401 / 6771	2	https://archive.ics.uci.edu/ml/datasets/thyroid+disease
Cervical Cancer	31	858	55 / 803	2	https://archive.ics.uci.edu/ml/datasets/Cervical+cancer+%28Risk+Factors%29
Spambase	57	4601	1813 / 2788	2	https://archive.ics.uci.edu/ml/datasets/spambase
Iris	4	150	50 / 50 / 50	3	https://archive.ics.uci.edu/ml/datasets/iris
Balance Scale	4	625	49 / 288 / 288	3	https://archive.ics.uci.edu/ml/datasets/balance+scale
Car	6	1728	384 / 69 / 1210 / 65	4	https://archive.ics.uci.edu/ml/datasets/car+evaluation
Glass	9	214	70 / 76 / 17 / 13 / 9 / 29	6	https://archive.ics.uci.edu/ml/datasets/glass+identification
Contraceptive	9	1473	629 / 333 / 511	3	https://archive.ics.uci.edu/ml/datasets/Contraceptive+Method+Choice
Solar Flare	10	1389	1171 / 141 / 40 / 20 / 9 / 4 / 3 / 1	8	http://archive.ics.uci.edu/ml/datasets/solar+flare
Wine	12	178	59 / 71 / 48	3	https://archive.ics.uci.edu/ml/datasets/wine
Zoo	16	101	41 / 20 / 5 / 13 / 4 / 8 / 10	7	https://archive.ics.uci.edu/ml/datasets/zoo
Lymphography	18	148	2 / 81 / 61 / 4	4	https://archive.ics.uci.edu/ml/datasets/Lymphography
Segment	19	2310	330 / 330 / 330 / 330 / 330	7	https://archive.ics.uci.edu/ml/datasets/image+segmentation
Dermatology	34	366	112 / 61 / 72 / 49 / 52 / 20	6	https://archive.ics.uci.edu/ml/datasets/dermatology
Landsat	36	6435	1533 / 703 / 1358 / 626 / 707 / 1508	6	https://archive.ics.uci.edu/ml/datasets/Statlog+(Landsat+Satellite)
Annealing	38	798	8 / 88 / 608 / 60 / 34	5	https://archive.ics.uci.edu/ml/datasets/Annealing
Splice	60	3190	767 / 768 / 1655	3	https://archive.ics.uci.edu/ml/datasets/Molecular+Biology+(Splice-junction+Gene+Sequences)

C Additional Results

Table 4: **Performance Comparison Default Hyperparameters.** We report macro F1-scores (mean \pm stdev over 10 trials) with default parameters. We also report the rank of each approach in brackets. The datasets are sorted by the number of features. The top part comprises binary classification tasks and the bottom part multi-class datasets.

	Gradient-Based		Non-Greedy		Greedy
	GDT (ours)	DNDT	GeneticTree	DL8.5	CART
Blood Transfusion	0.627 \pm 0.056 (1)	0.558 \pm 0.059 (5)	0.574 \pm 0.093 (3)	0.590 \pm 0.034 (2)	0.573 \pm 0.036 (4)
Banknote Authentication	0.980 \pm 0.008 (2)	0.886 \pm 0.024 (5)	0.928 \pm 0.022 (4)	0.962 \pm 0.011 (3)	0.981 \pm 0.006 (1)
Titanic	0.782 \pm 0.035 (1)	0.740 \pm 0.026 (4)	0.763 \pm 0.041 (2)	0.754 \pm 0.031 (3)	0.735 \pm 0.041 (5)
Raisins	0.850 \pm 0.025 (2)	0.832 \pm 0.026 (4)	0.859 \pm 0.022 (1)	0.849 \pm 0.027 (3)	0.811 \pm 0.028 (5)
Rice	0.926 \pm 0.006 (2)	0.902 \pm 0.018 (5)	0.927 \pm 0.005 (1)	0.925 \pm 0.008 (3)	0.905 \pm 0.010 (4)
Echocardiogram	0.648 \pm 0.130 (1)	0.543 \pm 0.117 (5)	0.563 \pm 0.099 (3)	0.609 \pm 0.112 (2)	0.559 \pm 0.075 (4)
Wisconsin Breast Cancer	0.902 \pm 0.029 (3)	0.907 \pm 0.037 (1)	0.888 \pm 0.021 (5)	0.896 \pm 0.021 (4)	0.904 \pm 0.025 (2)
Loan House	0.695 \pm 0.035 (1)	0.475 \pm 0.043 (4)	0.461 \pm 0.093 (5)	0.607 \pm 0.045 (3)	0.671 \pm 0.056 (2)
Heart Failure	0.745 \pm 0.063 (2)	0.580 \pm 0.077 (5)	0.740 \pm 0.055 (3)	0.692 \pm 0.062 (4)	0.755 \pm 0.060 (1)
Heart Disease	0.736 \pm 0.069 (1)	$n > 12$	0.704 \pm 0.059 (3)	0.722 \pm 0.065 (2)	0.670 \pm 0.090 (4)
Adult	0.749 \pm 0.028 (2)	$n > 12$	0.478 \pm 0.068 (4)	0.723 \pm 0.011 (3)	0.773 \pm 0.008 (1)
Bank Marketing	0.626 \pm 0.017 (1)	$n > 12$	0.473 \pm 0.002 (4)	0.502 \pm 0.011 (3)	0.616 \pm 0.007 (2)
Congressional Voting	0.953 \pm 0.021 (1)	$n > 12$	0.932 \pm 0.034 (3)	0.924 \pm 0.043 (4)	0.933 \pm 0.032 (2)
Absenteeism	0.620 \pm 0.050 (1)	$n > 12$	0.417 \pm 0.035 (4)	0.587 \pm 0.047 (2)	0.580 \pm 0.045 (3)
Hepatitis	0.609 \pm 0.103 (2)	$n > 12$	0.486 \pm 0.074 (4)	0.586 \pm 0.083 (3)	0.610 \pm 0.123 (1)
German	0.584 \pm 0.057 (2)	$n > 12$	0.412 \pm 0.005 (4)	0.556 \pm 0.035 (3)	0.595 \pm 0.028 (1)
Mushroom	0.997 \pm 0.003 (3)	$n > 12$	0.984 \pm 0.003 (4)	0.999 \pm 0.001 (1)	0.999 \pm 0.001 (2)
Credit Card	0.676 \pm 0.009 (4)	$n > 12$	0.685 \pm 0.004 (1)	0.679 \pm 0.007 (3)	0.679 \pm 0.007 (2)
Horse Colic	0.842 \pm 0.033 (1)	$n > 12$	0.794 \pm 0.042 (2)	0.708 \pm 0.038 (4)	0.758 \pm 0.053 (3)
Thyroid	0.872 \pm 0.015 (2)	$n > 12$	0.476 \pm 0.101 (4)	0.682 \pm 0.018 (3)	0.912 \pm 0.013 (1)
Cervical Cancer	0.496 \pm 0.047 (3)	$n > 12$	0.514 \pm 0.034 (1)	0.488 \pm 0.027 (4)	0.505 \pm 0.033 (2)
Spambase	0.893 \pm 0.015 (2)	$n > 12$	0.864 \pm 0.014 (3)	0.863 \pm 0.011 (4)	0.917 \pm 0.011 (1)
Mean	0.764 \pm 0.144 (1)	-	0.678 \pm 0.197 (4)	0.723 \pm 0.154 (3)	0.747 \pm 0.153 (2)
Mean Reciprocal Rank	0.670 \pm 0.289 (1)	0.306 \pm 0.262 (5)	0.427 \pm 0.287 (3)	0.371 \pm 0.164 (4)	0.571 \pm 0.318 (2)
Iris	0.938 \pm 0.039 (1)	0.870 \pm 0.051 (5)	0.912 \pm 0.038 (3)	0.909 \pm 0.046 (4)	0.937 \pm 0.036 (2)
Balance Scale	0.575 \pm 0.031 (2)	0.542 \pm 0.062 (3)	0.539 \pm 0.026 (4)	0.525 \pm 0.039 (5)	0.581 \pm 0.025 (1)
Car	0.389 \pm 0.062 (3)	0.426 \pm 0.065 (2)	0.321 \pm 0.069 (4)	0.273 \pm 0.063 (5)	0.571 \pm 0.133 (1)
Glass	0.484 \pm 0.099 (5)	0.498 \pm 0.096 (4)	0.566 \pm 0.152 (2)	0.501 \pm 0.100 (3)	0.668 \pm 0.085 (1)
Contraceptive	0.472 \pm 0.039 (1)	0.324 \pm 0.045 (3)	0.311 \pm 0.053 (4)	0.292 \pm 0.036 (5)	0.450 \pm 0.064 (2)
Solar Flare	0.145 \pm 0.017 (3)	0.142 \pm 0.025 (5)	0.150 \pm 0.026 (2)	0.144 \pm 0.034 (4)	0.180 \pm 0.026 (1)
Wine	0.895 \pm 0.035 (3)	0.853 \pm 0.042 (4)	0.898 \pm 0.041 (2)	0.852 \pm 0.022 (5)	0.907 \pm 0.042 (1)
Zoo	0.827 \pm 0.162 (3)	$n > 12$	0.802 \pm 0.094 (4)	0.911 \pm 0.106 (2)	0.943 \pm 0.076 (1)
Lymphography	0.472 \pm 0.192 (3)	$n > 12$	0.397 \pm 0.211 (4)	0.574 \pm 0.196 (2)	0.606 \pm 0.176 (1)
Segment	0.921 \pm 0.014 (2)	$n > 12$	0.736 \pm 0.064 (4)	0.808 \pm 0.013 (3)	0.950 \pm 0.006 (1)
Dermatology	0.876 \pm 0.041 (3)	$n > 12$	0.818 \pm 0.161 (4)	0.885 \pm 0.036 (2)	0.951 \pm 0.024 (1)
Landsat	0.791 \pm 0.012 (2)	$n > 12$	0.647 \pm 0.054 (4)	0.783 \pm 0.008 (3)	0.835 \pm 0.011 (1)
Annealing	0.632 \pm 0.155 (3)	$n > 12$	0.198 \pm 0.050 (4)	0.787 \pm 0.121 (2)	0.873 \pm 0.092 (1)
Splice	0.869 \pm 0.017 (2)	$n > 12$	0.611 \pm 0.095 (3)	> 60 min	0.878 \pm 0.028 (1)
Mean	0.638 \pm 0.244 (2)	-	0.565 \pm 0.256 (4)	0.634 \pm 0.268 (3)	0.738 \pm 0.235 (1)
Mean Reciprocal Rank	0.470 \pm 0.239 (2)	0.295 \pm 0.106 (5)	0.315 \pm 0.104 (4)	0.331 \pm 0.128 (3)	0.929 \pm 0.182 (1)

Table 5: **Train Performance Comparison.** We report macro F1-scores (mean \pm stdev over 10 trials) on the training data. We also report the rank of each approach in brackets. The datasets are sorted by the number of features. The top part comprises binary classification tasks and the bottom part multi-class datasets.

	Gradient-Based		Non-Greedy		Greedy
	GDT (ours)	DNDT	GeneticTree	DL8.5	CART
Blood Transfusion	0.686 \pm 0.032 (3)	0.552 \pm 0.085 (5)	0.615 \pm 0.122 (4)	0.711 \pm 0.045 (2)	0.832 \pm 0.040 (1)
Banknote Authentication	0.995 \pm 0.003 (2)	0.907 \pm 0.012 (5)	0.933 \pm 0.016 (4)	0.967 \pm 0.003 (3)	0.999 \pm 0.001 (1)
Titanic	0.761 \pm 0.128 (5)	0.791 \pm 0.025 (4)	0.908 \pm 0.023 (3)	0.970 \pm 0.006 (1)	0.949 \pm 0.012 (2)
Raisins	0.892 \pm 0.024 (1)	0.829 \pm 0.027 (5)	0.863 \pm 0.004 (4)	0.889 \pm 0.004 (2)	0.866 \pm 0.004 (3)
Rice	0.925 \pm 0.003 (3)	0.913 \pm 0.012 (5)	0.920 \pm 0.002 (4)	0.930 \pm 0.002 (1)	0.927 \pm 0.002 (2)
Echocardiogram	0.827 \pm 0.088 (4)	0.817 \pm 0.034 (5)	0.844 \pm 0.032 (3)	0.935 \pm 0.013 (2)	0.981 \pm 0.009 (1)
Wisconsin Breast Cancer	0.947 \pm 0.015 (2)	0.936 \pm 0.015 (3)	0.907 \pm 0.009 (5)	0.964 \pm 0.005 (1)	0.915 \pm 0.006 (4)
Loan House	0.735 \pm 0.009 (4)	0.712 \pm 0.010 (5)	0.897 \pm 0.012 (3)	0.969 \pm 0.006 (1)	0.938 \pm 0.009 (2)
Heart Failure	0.785 \pm 0.038 (4)	0.773 \pm 0.053 (5)	0.795 \pm 0.024 (3)	0.912 \pm 0.008 (1)	0.818 \pm 0.021 (2)
Heart Disease	0.851 \pm 0.027 (4)	$n > 12$	0.902 \pm 0.020 (3)	0.990 \pm 0.005 (1)	0.964 \pm 0.010 (2)
Adult	0.875 \pm 0.050 (4)	$n > 12$	0.932 \pm 0.013 (3)	0.967 \pm 0.001 (2)	0.973 \pm 0.001 (1)
Bank Marketing	0.603 \pm 0.029 (4)	$n > 12$	0.971 \pm 0.003 (3)	0.981 \pm 0.001 (2)	0.984 \pm 0.001 (1)
Congressional Voting	0.971 \pm 0.019 (4)	$n > 12$	0.978 \pm 0.005 (3)	1.000 \pm 0.001 (2)	1.000 \pm 0.000 (1)
Absenteeism	0.778 \pm 0.050 (4)	$n > 12$	0.842 \pm 0.011 (3)	0.920 \pm 0.009 (2)	0.952 \pm 0.008 (1)
Hepatitis	0.931 \pm 0.038 (4)	$n > 12$	0.967 \pm 0.011 (3)	1.000 \pm 0.000 (1)	0.998 \pm 0.003 (2)
German	0.589 \pm 0.048 (4)	$n > 12$	0.891 \pm 0.010 (3)	0.958 \pm 0.002 (1)	0.940 \pm 0.013 (2)
Mushroom	1.000 \pm 0.000 (1)	$n > 12$	0.993 \pm 0.005 (4)	1.000 \pm 0.000 (1)	1.000 \pm 0.000 (1)
Credit Card	0.651 \pm 0.020 (4)	$n > 12$	0.691 \pm 0.002 (3)	0.710 \pm 0.003 (2)	0.758 \pm 0.008 (1)
Horse Colic	0.882 \pm 0.033 (4)	$n > 12$	0.913 \pm 0.019 (3)	1.000 \pm 0.000 (1)	0.963 \pm 0.008 (2)
Thyroid	0.914 \pm 0.012 (4)	$n > 12$	0.927 \pm 0.014 (3)	0.937 \pm 0.002 (2)	0.987 \pm 0.002 (1)
Cervical Cancer	0.593 \pm 0.128 (4)	$n > 12$	0.691 \pm 0.046 (3)	0.767 \pm 0.020 (2)	0.925 \pm 0.027 (1)
Spambase	0.905 \pm 0.020 (2)	$n > 12$	0.858 \pm 0.020 (4)	0.879 \pm 0.002 (3)	0.965 \pm 0.003 (1)
Mean	0.823 \pm 0.132 (4)	-	0.874 \pm 0.098 (3)	0.925 \pm 0.087 (2)	0.938 \pm 0.065 (1)
Mean Reciprocal Rank	0.358 \pm 0.226 (3)	0.220 \pm 0.045 (5)	0.305 \pm 0.044 (4)	0.712 \pm 0.263 (2)	0.754 \pm 0.282 (1)
Iris	0.978 \pm 0.017 (2)	0.926 \pm 0.030 (5)	0.947 \pm 0.008 (4)	0.996 \pm 0.004 (1)	0.973 \pm 0.010 (3)
Balance Scale	0.793 \pm 0.034 (2)	0.602 \pm 0.142 (5)	0.665 \pm 0.034 (4)	0.700 \pm 0.022 (3)	0.932 \pm 0.010 (1)
Car	0.807 \pm 0.048 (4)	0.681 \pm 0.087 (5)	0.863 \pm 0.055 (3)	0.885 \pm 0.029 (2)	0.974 \pm 0.010 (1)
Glass	0.785 \pm 0.045 (4)	0.804 \pm 0.020 (3)	0.699 \pm 0.049 (5)	0.837 \pm 0.009 (2)	0.978 \pm 0.007 (1)
Contraceptive	0.545 \pm 0.067 (5)	0.591 \pm 0.105 (4)	0.723 \pm 0.030 (3)	0.822 \pm 0.016 (2)	0.865 \pm 0.018 (1)
Solar Flare	0.833 \pm 0.090 (3)	0.729 \pm 0.080 (5)	0.794 \pm 0.123 (4)	0.904 \pm 0.047 (2)	0.943 \pm 0.061 (1)
Wine	0.995 \pm 0.009 (3)	0.996 \pm 0.006 (2)	0.931 \pm 0.019 (5)	0.978 \pm 0.004 (4)	1.000 \pm 0.000 (1)
Zoo	0.990 \pm 0.029 (3)	$n > 12$	0.831 \pm 0.129 (4)	1.000 \pm 0.000 (1)	1.000 \pm 0.000 (2)
Lymphography	0.974 \pm 0.018 (2)	$n > 12$	0.915 \pm 0.072 (4)	0.957 \pm 0.130 (3)	0.988 \pm 0.004 (1)
Segment	0.959 \pm 0.005 (2)	$n > 12$	0.715 \pm 0.109 (4)	0.799 \pm 0.003 (3)	0.987 \pm 0.002 (1)
Dermatology	0.965 \pm 0.014 (2)	$n > 12$	0.792 \pm 0.110 (4)	0.954 \pm 0.007 (3)	0.986 \pm 0.005 (1)
Landsat	0.824 \pm 0.010 (2)	$n > 12$	0.630 \pm 0.083 (4)	0.792 \pm 0.004 (3)	0.939 \pm 0.005 (1)
Annealing	0.885 \pm 0.089 (4)	$n > 12$	0.974 \pm 0.013 (3)	0.999 \pm 0.001 (2)	0.999 \pm 0.001 (1)
Splice	0.886 \pm 0.026 (2)	$n > 12$	0.783 \pm 0.062 (3)	> 60 min	0.992 \pm 0.004 (1)
Mean	0.873 \pm 0.123 (3)	-	0.804 \pm 0.110 (4)	0.894 \pm 0.097 (2)	0.968 \pm 0.038 (1)
Mean Reciprocal Rank	0.389 \pm 0.121 (3)	0.269 \pm 0.113 (4)	0.267 \pm 0.047 (5)	0.494 \pm 0.242 (2)	0.952 \pm 0.178 (1)

Table 6: **Tree Size Comparison.** We report the average tree size based on the optimized hyperparameters (mean \pm stdev over 10 trials). We also report the rank of each approach in brackets. The datasets are sorted by the number of features. The top part comprises binary classification tasks and the bottom part multi-class datasets.

	Gradient-Based				Non-Greedy				Greedy	
	GDT (ours)		DNDT		GeneticTree		DL8.5		CART	
Blood Transfusion	29.200 \pm 8.219 (3)	24.000 \pm 0.000 (2)	5.200 \pm 3.027 (1)	24.000 \pm 1.612 (3)	165.600 \pm 21.837 (5)					
Banknote Authentication	60.000 \pm 11.216 (5)	24.000 \pm 0.000 (2)	12.800 \pm 5.325 (1)	26.800 \pm 0.600 (3)	44.800 \pm 4.686 (4)					
Titanic	39.600 \pm 10.161 (3)	142.000 \pm 0.000 (5)	10.400 \pm 3.105 (1)	28.200 \pm 0.980 (3)	21.600 \pm 0.917 (2)					
Raisins	114.800 \pm 33.686 (4)	142.000 \pm 0.000 (5)	3.600 \pm 1.800 (2)	29.400 \pm 1.497 (3)	3.000 \pm 0.000 (1)					
Rice	41.000 \pm 10.040 (4)	142.000 \pm 0.000 (5)	3.000 \pm 0.000 (2)	30.200 \pm 0.980 (3)	3.000 \pm 0.000 (1)					
Echocardiogram	43.200 \pm 12.820 (4)	272.000 \pm 0.000 (5)	9.000 \pm 3.098 (1)	30.000 \pm 1.342 (2)	36.200 \pm 5.810 (3)					
Wisconsin Breast Cancer	61.800 \pm 13.363 (4)	1,044.000 \pm 0.000 (5)	4.000 \pm 1.612 (2)	29.400 \pm 0.800 (3)	3.000 \pm 0.000 (1)					
Loan House	19.200 \pm 5.250 (2)	2,070.000 \pm 0.000 (5)	6.800 \pm 2.750 (1)	28.200 \pm 1.327 (4)	26.200 \pm 2.040 (3)					
Heart Failure	27.200 \pm 9.442 (3)	4,120.000 \pm 0.000 (5)	3.200 \pm 0.600 (1)	30.800 \pm 0.600 (4)	14.200 \pm 0.980 (2)					
Heart Disease	36.800 \pm 7.454 (4)	$n > 12$	11.000 \pm 4.099 (1)	27.600 \pm 1.562 (3)	24.600 \pm 3.072 (2)					
Adult	128.000 \pm 37.194 (3)	$n > 12$	9.400 \pm 4.964 (1)	25.200 \pm 0.600 (2)	156.600 \pm 23.079 (4)					
Bank Marketing	6.800 \pm 3.027 (2)	$n > 12$	3.400 \pm 1.200 (1)	27.200 \pm 2.272 (3)	110.600 \pm 10.500 (1)					
Congressional Voting	5.600 \pm 2.375 (2)	$n > 12$	5.600 \pm 0.917 (1)	20.400 \pm 6.696 (4)	19.200 \pm 6.416 (3)					
Absenteeism	148.800 \pm 18.187 (4)	$n > 12$	7.800 \pm 0.980 (1)	30.600 \pm 0.800 (2)	43.200 \pm 2.750 (3)					
Hepatitis	12.200 \pm 3.600 (2)	$n > 12$	5.800 \pm 2.713 (1)	14.800 \pm 2.088 (4)	12.600 \pm 1.744 (3)					
German	27.600 \pm 4.104 (2)	$n > 12$	6.200 \pm 0.980 (1)	30.400 \pm 0.917 (3)	34.600 \pm 5.713 (4)					
Mushroom	25.600 \pm 5.731 (4)	$n > 12$	5.200 \pm 1.661 (1)	21.200 \pm 2.750 (3)	14.000 \pm 1.342 (2)					
Credit Card	92.600 \pm 39.636 (3)	$n > 12$	3.000 \pm 0.000 (1)	31.000 \pm 0.000 (2)	354.800 \pm 31.603 (4)					
Horse Colic	22.400 \pm 4.737 (3)	$n > 12$	4.000 \pm 1.612 (1)	29.400 \pm 1.200 (4)	12.600 \pm 1.200 (2)					
Thyroid	96.800 \pm 16.863 (4)	$n > 12$	5.600 \pm 1.800 (1)	30.600 \pm 0.800 (2)	66.400 \pm 4.652 (3)					
Cervical Cancer	34.000 \pm 23.669 (3)	$n > 12$	14.000 \pm 7.550 (1)	30.800 \pm 0.600 (2)	99.000 \pm 8.532 (4)					
Spambase	120.200 \pm 37.010 (3)	$n > 12$	12.400 \pm 5.800 (1)	29.600 \pm 0.917 (2)	201.000 \pm 14.642 (4)					
Mean	54.245 \pm 42.824 (3)	886.667 \pm 1,387.861 (5)	6.882 \pm 3.457 (1)	27.536 \pm 4.146 (2)	66.673 \pm 86.224 (4)					
Mean Reciprocal Rank	0.331 \pm 0.102 (4)	0.267 \pm 0.132 (5)	0.932 \pm 0.176 (1)	0.367 \pm 0.098 (3)	0.430 \pm 0.252 (2)					
Iris	14.400 \pm 2.538 (3)	24.000 \pm 0.000 (4)	9.000 \pm 3.098 (1)	29.200 \pm 1.400 (5)	9.400 \pm 1.497 (2)					
Balance Scale	118.600 \pm 27.097 (4)	24.000 \pm 0.000 (1)	25.400 \pm 11.307 (2)	31.000 \pm 0.000 (3)	161.200 \pm 8.920 (5)					
Car	47.000 \pm 13.565 (3)	76.000 \pm 0.000 (5)	32.600 \pm 21.350 (1)	29.800 \pm 0.980 (2)	57.000 \pm 13.023 (4)					
Glass	56.800 \pm 11.007 (3)	530.000 \pm 0.000 (5)	21.800 \pm 11.531 (1)	30.600 \pm 0.800 (2)	68.000 \pm 6.340 (4)					
Contraceptive	40.600 \pm 11.482 (3)	530.000 \pm 0.000 (5)	12.800 \pm 3.842 (1)	30.000 \pm 1.342 (2)	48.600 \pm 7.144 (4)					
Solar Flare	49.800 \pm 9.304 (4)	1,044.000 \pm 0.000 (5)	38.400 \pm 21.411 (3)	26.800 \pm 3.280 (1)	32.000 \pm 3.130 (2)					
Wine	24.000 \pm 4.123 (3)	4,120.000 \pm 0.000 (5)	11.200 \pm 4.771 (1)	28.200 \pm 1.600 (4)	13.400 \pm 2.332 (2)					
Zoo	25.000 \pm 3.899 (3)	$n > 12$	32.600 \pm 19.304 (4)	24.600 \pm 0.800 (2)	18.000 \pm 1.342 (1)					
Lymphography	36.200 \pm 6.337 (4)	$n > 12$	14.400 \pm 6.815 (1)	27.000 \pm 1.265 (3)	16.800 \pm 1.887 (2)					
Segment	133.000 \pm 21.854 (4)	$n > 12$	24.400 \pm 11.421 (1)	31.000 \pm 0.000 (2)	79.600 \pm 3.800 (3)					
Dermatology	33.600 \pm 7.269 (4)	$n > 12$	20.000 \pm 7.759 (1)	28.000 \pm 1.844 (2)	28.000 \pm 1.844 (2)					
Landsat	360.600 \pm 21.124 (3)	$n > 12$	16.000 \pm 7.335 (1)	31.000 \pm 0.000 (2)	425.600 \pm 18.527 (4)					
Annealing	19.600 \pm 2.835 (2)	$n > 12$	12.600 \pm 3.323 (1)	28.400 \pm 2.010 (4)	24.400 \pm 2.010 (3)					
Splice	247.400 \pm 52.997 (3)	$n > 12$	11.800 \pm 6.400 (1)	$n > 12$	81.400 \pm 10.688 (2)					
Mean	86.186 \pm 101.070 (4)	906.857 \pm 1,464.942 (5)	20.214 \pm 9.310 (1)	28.946 \pm 1.983 (2)	75.957 \pm 108.423 (3)					
Mean Reciprocal Rank	0.315 \pm 0.067 (5)	0.321 \pm 0.300 (4)	0.863 \pm 0.277 (1)	0.451 \pm 0.202 (2)	0.419 \pm 0.206 (3)					

Table 7: **Runtime Comparison.** We report runtime without restarts based on the optimized hyperparameters (mean \pm stdev over 10 trials). We also report the rank of each approach in brackets. The datasets are sorted by the number of features. The top part comprises binary classification tasks and the bottom part multi-class datasets.

	Gradient-Based		Non-Greedy		Greedy
	GDT (ours)	DNDT	GeneticTree	DL8.5	CART
Blood Transfusion	13.007 \pm 1.000 (5)	3.704 \pm 1.000 (3)	10.514 \pm 4.000 (4)	0.031 \pm 0.000 (2)	0.002 \pm 0.000 (1)
Banknote Authentication	13.209 \pm 2.000 (4)	34.425 \pm 1.000 (5)	10.318 \pm 3.000 (3)	0.025 \pm 0.000 (2)	0.003 \pm 0.000 (1)
Titanic	29.579 \pm 1.000 (5)	6.815 \pm 0.000 (4)	3.677 \pm 1.000 (3)	0.259 \pm 0.000 (2)	0.002 \pm 0.000 (1)
Raisins	30.611 \pm 2.000 (5)	8.495 \pm 1.000 (4)	0.619 \pm 0.000 (3)	0.198 \pm 0.000 (2)	0.004 \pm 0.000 (1)
Rice	21.487 \pm 4.000 (5)	11.955 \pm 1.000 (4)	1.329 \pm 0.000 (3)	0.475 \pm 0.000 (2)	0.013 \pm 0.000 (1)
Echocardiogram	9.038 \pm 1.000 (4)	9.564 \pm 2.000 (5)	0.304 \pm 0.000 (3)	0.093 \pm 0.000 (2)	0.002 \pm 0.000 (1)
Wisconsin Breast Cancer	29.246 \pm 2.000 (5)	6.837 \pm 1.000 (4)	1.187 \pm 0.000 (3)	0.461 \pm 0.000 (2)	0.003 \pm 0.000 (1)
Loan House	10.798 \pm 1.000 (4)	52.793 \pm 7.000 (5)	6.751 \pm 2.000 (3)	0.524 \pm 0.000 (2)	0.002 \pm 0.000 (1)
Heart Failure	28.395 \pm 1.000 (5)	23.747 \pm 10.000 (4)	1.473 \pm 0.000 (3)	0.201 \pm 0.000 (2)	0.002 \pm 0.000 (1)
Heart Disease	15.565 \pm 2.000 (4)	$n > 12$	4.446 \pm 1.000 (3)	0.636 \pm 0.000 (2)	0.002 \pm 0.000 (1)
Adult	86.241 \pm 12.000 (4)	$n > 12$	26.012 \pm 7.000 (3)	22.321 \pm 1.000 (2)	0.071 \pm 0.000 (1)
Bank Marketing	153.494 \pm 38.000 (4)	$n > 12$	129.428 \pm 8.000 (3)	54.545 \pm 1.000 (2)	0.072 \pm 0.000 (1)
Congressional Voting	32.935 \pm 3.000 (4)	$n > 12$	6.503 \pm 1.000 (3)	4.100 \pm 7.000 (2)	0.002 \pm 0.000 (1)
Absenteeism	28.941 \pm 1.000 (4)	$n > 12$	14.045 \pm 3.000 (3)	3.893 \pm 0.000 (2)	0.003 \pm 0.000 (1)
Hepatitis	28.427 \pm 1.000 (4)	$n > 12$	2.273 \pm 1.000 (3)	0.023 \pm 0.000 (2)	0.002 \pm 0.000 (1)
German	12.307 \pm 2.000 (4)	$n > 12$	3.141 \pm 1.000 (2)	10.288 \pm 0.000 (3)	0.003 \pm 0.000 (1)
Mushroom	58.810 \pm 70.000 (4)	$n > 12$	12.507 \pm 2.000 (3)	0.507 \pm 0.000 (2)	0.007 \pm 0.000 (1)
Credit Card	111.425 \pm 36.000 (3)	$n > 12$	4.416 \pm 0.000 (2)	298.572 \pm 6.000 (4)	0.351 \pm 0.000 (1)
Horse Colic	9.811 \pm 1.000 (4)	$n > 12$	0.316 \pm 0.000 (2)	2.365 \pm 2.000 (3)	0.002 \pm 0.000 (1)
Thyroid	35.965 \pm 13.000 (2)	$n > 12$	38.287 \pm 15.000 (3)	109.123 \pm 3.000 (4)	0.013 \pm 0.000 (1)
Cervical Cancer	13.465 \pm 2.000 (4)	$n > 12$	2.760 \pm 1.000 (3)	0.126 \pm 0.000 (2)	0.006 \pm 0.000 (1)
Spambase	41.983 \pm 5.000 (4)	$n > 12$	19.289 \pm 6.000 (3)	4.576 \pm 0.000 (2)	0.036 \pm 0.000 (1)
Mean	44.745 \pm 38.655 (4)	-	13.618 \pm 27.539 (2)	23.334 \pm 66.445 (3)	0.027 \pm 0.075 (1)
Mean Reciprocal Rank	0.244 \pm 0.037 (4)	0.243 \pm 0.042 (5)	0.352 \pm 0.063 (3)	0.462 \pm 0.084 (2)	1.000 \pm 1.000 (1)
Iris	7.245 \pm 1.000 (5)	2.959 \pm 0.000 (4)	0.968 \pm 0.000 (3)	0.016 \pm 0.000 (2)	0.001 \pm 0.000 (1)
Balance Scale	11.614 \pm 2.000 (5)	10.123 \pm 9.000 (4)	8.180 \pm 1.000 (3)	0.038 \pm 0.000 (2)	0.002 \pm 0.000 (1)
Car	23.721 \pm 3.000 (3)	46.910 \pm 43.000 (5)	29.688 \pm 10.000 (4)	0.239 \pm 0.000 (2)	0.005 \pm 0.000 (1)
Glass	30.142 \pm 2.000 (5)	5.486 \pm 0.000 (3)	12.975 \pm 5.000 (4)	0.180 \pm 0.000 (2)	0.002 \pm 0.000 (1)
Contraceptive	13.165 \pm 2.000 (5)	12.670 \pm 2.000 (4)	3.952 \pm 1.000 (3)	0.262 \pm 0.000 (2)	0.003 \pm 0.000 (1)
Solar Flare	22.108 \pm 2.000 (4)	25.652 \pm 3.000 (5)	14.733 \pm 2.000 (3)	0.544 \pm 0.000 (2)	0.004 \pm 0.000 (1)
Wine	30.096 \pm 1.000 (4)	58.486 \pm 10.000 (5)	0.128 \pm 0.000 (2)	0.543 \pm 0.000 (3)	0.002 \pm 0.000 (1)
Zoo	19.259 \pm 7.000 (4)	$n > 12$	9.560 \pm 3.000 (3)	0.015 \pm 0.000 (2)	0.002 \pm 0.000 (1)
Lymphography	7.890 \pm 1.000 (4)	$n > 12$	4.359 \pm 1.000 (3)	0.143 \pm 0.000 (2)	0.002 \pm 0.000 (1)
Segment	16.178 \pm 3.000 (4)	$n > 12$	2.967 \pm 1.000 (2)	14.315 \pm 1.000 (3)	0.016 \pm 0.000 (1)
Dermatology	9.909 \pm 3.000 (3)	$n > 12$	1.722 \pm 1.000 (2)	20.708 \pm 6.000 (4)	0.003 \pm 0.000 (1)
Landsat	38.134 \pm 11.000 (3)	$n > 12$	33.831 \pm 11.000 (2)	830.055 \pm 9.000 (4)	0.052 \pm 0.000 (1)
Annealing	36.187 \pm 3.000 (3)	$n > 12$	1.364 \pm 0.000 (2)	104.566 \pm 24.000 (4)	0.007 \pm 0.000 (1)
Splice	19.203 \pm 2.000 (3)	$n > 12$	2.877 \pm 1.000 (2)	> 60 min	0.019 \pm 0.000 (1)
Mean	20.347 \pm 10.214 (3)	-	9.093 \pm 10.632 (2)	74.740 \pm 228.754 (4)	0.009 \pm 0.014 (1)
Mean Reciprocal Rank	0.266 \pm 0.056 (4)	0.241 \pm 0.048 (5)	0.393 \pm 0.100 (2)	0.383 \pm 0.126 (3)	1.000 \pm 1.000 (1)

D Hyperparameters

In the following, we report the hyperparameters used for each approach. The hyperparameters were selected based on a random search over a predefined parameter range for GDT, CART and GeneticTree and are summarized in Table 8 to Table 11. All parameters that were considered are noted in the tables. The number of trials was equal for each approach. For GDT and DNDT, we did not optimize the batch size as well as the number of epochs, but used early stopping with a predefined patience of 200. Additionally, we used 3 random restarts to prevent bad initial parametrizations and selected the best model based on the validation loss. A gradient-based optimization allows using an arbitrary loss function for the optimization. During preliminary experiments, we observed that it is beneficial to adjust the loss function for specific datasets. More specifically, we considered the binary crossentropy and the focal loss [22] with a focal factor of 3. Additionally, we considered using PolyLoss [20] within the HPO to tailor the loss function for the specific task. For DL8.5 there are no tunable hyperparameters except the maximum depth. However, the maximum depth strongly impacts the runtime, which is why we fixed the maximum depth to 4, similar to the maximum depth used during the experiments of Demirović et al. [10] and Aglin et al. [3]. Running the experiments with a higher depth becomes infeasible for many datasets. In preliminary experiments, we also observed that increasing the depth to 5 results in a decrease in the test performance. For DNDT, the number of cut points is the tunable hyperparameter of the model, according to Yang et al. [37]. However, it has to be restricted to 1 in order to generate binary trees for comparability reasons. Therefore, we only optimized the temperature and the learning rate. Furthermore, we extended their implementation to use early stopping based on the validation loss, similar to GDTs, to reduce the runtime and prevent overfitting. Further details can be found in the code, which we provided in the Appendix D.

Table 8: GDT Hyperparameters

Dataset Name	depth	lr_index	lr_values	lr_leaf	index_activation	loss	polyLoss	polyLossEpsilon
Blood Transfusion	8	0.010	0.100	0.010	entmax	crossentropy	False	2
Banknote Authentication	7	0.050	0.050	0.100	entmax	focal_crossentropy	True	2
Titanic	10	0.005	0.010	0.010	entmax	crossentropy	False	2
Raisins	10	0.005	0.005	0.100	entmax	crossentropy	True	5
Rice	7	0.050	0.010	0.010	entmax	crossentropy	False	2
Echocardiogram	8	0.010	0.050	0.100	entmax	crossentropy	True	5
Wisconsin Diagnostic Breast Cancer	10	0.050	0.010	0.100	entmax	crossentropy	True	2
Loan House	8	0.005	0.100	0.010	entmax	focal_crossentropy	False	2
Heart Failure	10	0.005	0.250	0.100	entmax	crossentropy	False	2
Heart Disease	9	0.010	0.050	0.005	entmax	focal_crossentropy	False	2
Adult	8	0.050	0.005	0.050	entmax	crossentropy	True	5
Bank Marketing	8	0.250	0.250	0.050	entmax	crossentropy	False	2
Cervical Cancer	8	0.005	0.010	0.100	entmax	crossentropy	True	2
Congressional Voting	10	0.005	0.050	0.010	entmax	focal_crossentropy	True	5
Absenteeism	10	0.050	0.010	0.050	entmax	focal_crossentropy	True	5
Hepatitis	10	0.005	0.050	0.010	entmax	focal_crossentropy	True	5
German	7	0.005	0.050	0.010	entmax	crossentropy	True	2
Mushroom	9	0.010	0.010	0.050	entmax	focal_crossentropy	False	2
Credit Card	8	0.050	0.100	0.010	entmax	focal_crossentropy	False	2
Horse Colic	8	0.250	0.250	0.010	entmax	focal_crossentropy	False	2
Thyroid	8	0.010	0.010	0.050	entmax	crossentropy	False	2
Spambase	10	0.005	0.010	0.010	entmax	crossentropy	False	2
Iris	7	0.005	0.005	0.05	entmax	crossentropy	False	2
Balance Scale	8	0.050	0.010	0.10	entmax	crossentropy	True	5
Car	9	0.010	0.010	0.01	entmax	focal_crossentropy	False	2
Glass	10	0.050	0.050	0.05	entmax	focal_crossentropy	True	5
Contraceptive	7	0.010	0.050	0.01	entmax	crossentropy	False	2
Solar Flare	8	0.005	0.010	0.20	entmax	focal_crossentropy	True	2
Wine	10	0.010	0.050	0.01	entmax	focal_crossentropy	False	2
Zoo	9	0.050	0.010	0.10	entmax	focal_crossentropy	True	2
Lymphography	8	0.050	0.010	0.05	entmax	crossentropy	True	2
Segment	7	0.005	0.005	0.05	entmax	crossentropy	False	2
Dermatology	7	0.010	0.010	0.10	entmax	crossentropy	True	2
Landsat	8	0.005	0.010	0.05	entmax	crossentropy	True	5
Annealing	10	0.250	0.050	0.01	entmax	crossentropy	False	2
Splice	9	0.010	0.005	0.05	entmax	crossentropy	False	2

Table 9: DNDT Hyperparameters

Dataset Name	learning_rate	temperature	num_cut
Blood Transfusion	0.050	0.100	1
Banknote Authentication	0.001	0.100	1
Titanic	0.050	0.001	1
Raisins	0.050	0.001	1
Rice	0.100	0.010	1
Echocardiogram	0.005	1.000	1
Wisconsin Diagnostic Breast Cancer	0.100	0.010	1
Loan House	0.001	1.000	1
Heart Failure	0.005	1.000	1
Iris	0.050	0.100	1
Balance Scale	0.005	0.100	1
Car	0.010	0.010	1
Glass	0.100	0.010	1
Contraceptive	0.001	0.010	1
Solar Flare	0.050	0.100	1
Wine	0.001	0.100	1

Table 10: GeneticTree Hyperparameters

Dataset Name	n_thresholds	n_trees	max_iter	cross_prob	mutation_prob
Blood Transfusion	10	500	500	1.0	0.2
Banknote Authentication	10	500	500	0.8	0.6
Titanic	10	500	250	0.2	0.3
Raisins	10	100	50	1.0	0.6
Rice	10	100	250	0.4	0.3
Echocardiogram	10	50	100	0.8	0.4
Wisconsin Diagnostic Breast Cancer	10	250	100	0.2	0.7
Loan House	10	500	500	1.0	0.2
Heart Failure	10	500	50	0.4	0.6
Heart Disease	10	400	500	0.6	0.4
Adult	10	100	500	0.6	0.6
Bank Marketing	10	500	250	0.8	0.6
Cervical Cancer	10	100	500	0.4	0.9
Congressional Voting	10	500	500	1.0	0.7
Absenteeism	10	500	500	1.0	0.7
Hepatitis	10	500	250	0.2	0.3
German	10	250	500	0.4	0.8
Mushroom	10	400	500	0.6	0.4
Credit Card	10	50	50	0.4	0.1
Horse Colic	10	50	100	0.8	0.4
Thyroid	10	500	500	1.0	0.7
Spambase	10	250	500	0.8	0.6
Iris	10	100	500	1.0	0.5
Balance Scale	10	500	250	0.6	0.4
Car	10	500	500	1.0	0.7
Glass	10	500	500	0.8	0.6
Contraceptive	10	250	500	0.4	0.5
Solar Flare	10	500	250	0.6	0.4
Wine	10	100	50	0.2	0.8
Zoo	10	500	500	1.0	0.7
Lymphography	10	500	250	0.6	0.4
Segment	10	100	500	0.4	0.9
Dermatology	10	100	500	1.0	0.5
Landsat	10	500	500	1.0	0.7
Annealing	10	100	500	0.4	0.9
Splice	10	100	250	0.2	0.8

Table 11: CART Hyperparameters

Dataset Name	max_depth	criterion	max_features	min_samples_leaf	min_samples_split	ccp_alpha
Blood Transfusion	9	entropy	None	1	5	0.0
Banknote Authentication	9	gini	None	1	5	0.0
Titanic	7	entropy	None	1	50	0.0
Raisins	8	gini	None	5	2	0.2
Rice	8	gini	None	5	2	0.2
Echocardiogram	9	entropy	None	1	5	0.0
Wisconsin Breast Cancer	7	entropy	None	5	2	0.4
Loan House	10	entropy	None	10	2	0.0
Heart Failure	9	gini	None	5	50	0.0
Heart Disease	8	entropy	None	5	10	0.0
Adult	10	entropy	None	10	2	0.0
Bank Marketing	8	entropy	None	5	10	0.0
Cervical Cancer	9	entropy	None	1	5	0.0
Congressional Voting	10	gini	None	1	2	0.0
Absenteeism	7	entropy	None	1	10	0.0
Hepatitis	9	entropy	None	1	5	0.0
German	7	entropy	None	1	10	0.0
Mushroom	9	entropy	None	1	5	0.0
Credit Card	9	gini	None	1	5	0.0
Horse Colic	10	entropy	None	10	2	0.0
Thyroid	10	entropy	None	10	2	0.0
Spambase	10	gini	None	1	2	0.0
Iris	8	entropy	None	5	10	0.0
Balance Scale	9	entropy	None	1	5	0.0
Car	9	gini	None	1	5	0.0
Glass	9	gini	None	1	5	0.0
Contraceptive	9	entropy	None	1	5	0.0
Solar Flare	7	entropy	None	1	50	0.0
Wine	9	gini	None	1	5	0.0
Zoo	10	gini	None	1	2	0.0
Lymphography	7	entropy	None	1	10	0.0
Segment	9	entropy	None	1	5	0.0
Dermatology	9	gini	None	1	5	0.0
Landsat	10	gini	None	1	2	0.0
Annealing	9	gini	None	1	5	0.0
Splice	9	gini	None	1	5	0.0